2021

Albatross and Falcon inspired Bionic UAV: An Aerodynamic Analysis

Bilji C. Mathew
Lovely Professional University, biljicm@gmail.com
Sagar K. Sahu
Lovely Professional University, sagar.sahu.0411@gmail.com
Prantik Dutta
Lovely Professional University, dutta.prantik13@gmail.com
Rushi Savale
Lovely professional university, rushisavale007@gmail.com
Muruga Lal Jeyan JV Dr.
Lovely professional University, jvmlal@ymail.com

Follow this and additional works at: https://commons.erau.edu/ijaaa

Part of the Aerodynamics and Fluid Mechanics Commons, and the Aeronautical Vehicles Commons

Albatross and Falcon inspired Bionic UAV: An Aerodynamic Analysis

The planform of any wing (Thomas et al., 2010) and its performance depends on the bird's genetic encoding and its degree of evolution in order to adapt to its niche. Pressure differences between the dorsal and ventral side of a wing is the reason behind lift generation. Different types of drag act on the bird's body during different modes of flight. A hereditary countering mechanism helps them to minimize the adverse effects of drag. This is inherent and differs from one species to another. The albatross is a large seabird capable of soaring miles without having to land. Its wingtips are pointed and the wing is characterized by higher values of aspect ratio (AR), lift to drag (L/D) ratio, and wing loading (W/S). No deflections are observed on the tips of an albatross's wing whilst soaring which is uncharacteristic for a planform having an elliptical lift distribution (ELD). This can be explained by a different type of lift distribution called the bell shaped lift distribution (BSLD) which unlike the ELD does not exhibit a total and constant downwash from root to tip. Ludwig Prandtl's works on BSLD has been very instrumental. Apart from some special cases (Hunsaker & Phillips, 2020) where ELD does provide optimum results, BSLD proves to be a more efficient type of lift distribution due to a tapering lift value as we move span-wise from root to tips.

Purpose

The purpose of this study was to mimic the albatross's and the falcon's aerodynamic qualities and exploit them to obtain a design that could act as a base for further designs involving bionic drones with optimum aerodynamic properties and low energy dissipation.

Literature Review

Ludwig Prandtl's (Newton, 2019) solution of minimum induced drag (Di) that involved a wing whose mass was considered constrained, exhibited the following properties-

1. The facility of an increased span of 22% whilst having 11% less Di acting on the wing
2. Upwash was observed on the wings due to tapering lift values at wingtips of the wing
3. A counter measure against adverse yaw was observed which can be referred to as the Proverse Yaw
4. A stable tailless flight can be observed

Figure 1

Comparison Between an Elliptical and a Bell ShapedLift Distribution
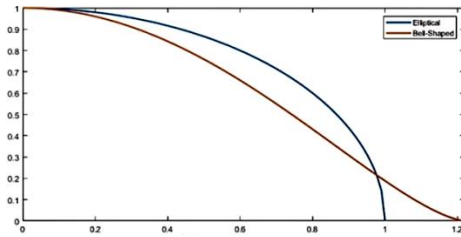
(a)Fraction of Maximum Lift vs Fraction of Elliptically Loaded Wing Length
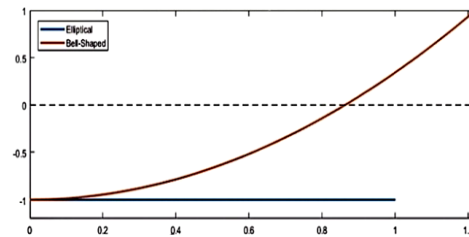
(b)Fraction of Maximum Downwash vs Fraction of Elliptically Loaded Wing Length

Despite having a tailless (Richter et al., n.d.) configuration, flying wings exhibit increased efficiency. Design parameters such as adding a sweep angle must be undertaken for efficiency. This in turn does increase the Di as well. Therefore even after observing a trend of increased longitudinal and directional stability the overall net performance exhibits decreased vales. One such solution to this complication is the BSLD which has an inherent proverse yaw property. One more important property (Bowers et al., 2016) of the BSLD is shedding of vortices which unlike the ELD occur at around 70% of the wingspan which implies that the magnitude of load acting on the tips of the wing is virtually zero. This explains as to why deflections are not observed on the wingtips of an albatross in soaring flight mode. A transition trend is observed from downwash to upwash for a wing with BSLD and this is the reason behind tapering lift values spanwise and zero loads acting on the tips of the wing.

Figure 2

Upwash and Downwash of Elliptical and Bell Span loads of Ludwig Prandtl
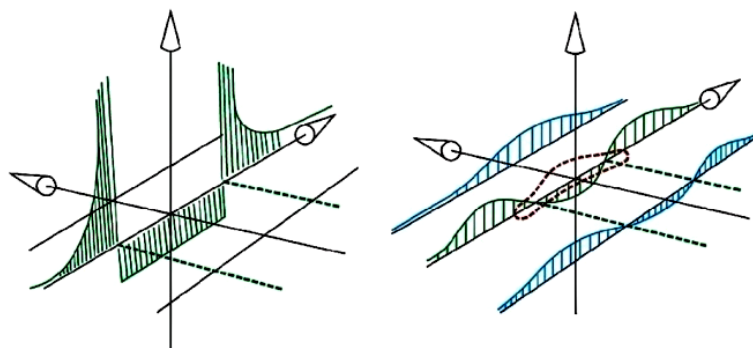
Rectangular and trapezoidal wings (Hospodář & Drábek, n.d.) are characterized by comparatively higher values of drag than wings having a BSLD. Even though rectangular wings are easier to manufacture, they exhibit higher values of drag since they have higher AR and even at lower values of speed, a rectangular wing requires to cruise at a higher angle of attack (AoA).Curling of high pressure air (Panagiotou et al., 2017) from the lower side due the pressure difference leads to the formation of wingtip vortices.

Based on turbulent boundary layer (Nielsen & Schwind, 1971) we can divide the vortex layer into three regions- inner region which is referred to as the vortex core, the logarithmic region and the defect low region. At lower angles of attack, very negligible generation of wingtip vortices is observed due to low pressure imbalance but the trend changes as we keep varying the angle of attack. A winglet can reduce the size and magnitude of vortices by reducing vorticity in the core and by reshaping the wake.

The inherent evolutionary wing colours (Hassanalian et al., 2017a) of an albatross is one of the main reasons behind the higher values of endurance exhibited by the bird. This is mainly due to the fact that a difference in the heat absorbed by the upper and the lower wing surface of the albatross is observed which in turn is characterized by lower drag values. Darker colours, mostly black, on the tips of the wings are for higher values of strength which can be seen when no deflections are observed during the soaring flight of an albatross. These wings also exhibit higher values of AR, W/S, and L/D ratio. The upper and lower surfaces of the wing are generally black and white in colour, respectively (Hassanalian, Throneberry, et al., 2018a). These are subjected to different types of radiations under different weather conditions during different times in a day. This in turn influences as to how the heat is absorbed by both the surfaces.

Varying temperature on both surfaces (Hassanalian et al., 2018a) is due to different rates at which heat is being absorbed by both the upper and the lower surface. Darker colours tend to absorb heat more effectively while lighter colours exhibit a reverse trend. During the day the upper wing surface which is black in colour is exposed to atmospheric and solar radiations while the lower surface which is white in colour is exposed to atmospheric and oceanic radiations. This means the rate of heat absorption will be higher in the upper region as compared to the lower region. This implies that a temperature difference will be observed with the upper region exhibiting higher values of temperature. This helps in reduction of the skin friction drag in the upper region. Due to the absence of solar radiations, this trend is reversed during the night. But despite this fact, the overall net drag reduction values will be high as these migratory birds migrate to regions with warmer climates. Also, these birds tend to travel less at night. Solving the values of drag (Hassanalian et al., 2017b) with Blasius solution for heated boundary layer gave a difference in the rates of heat absorption by the darker and

lighter wing regions. It was approximately 283K. Also varying the colours of the wings from lighter shades of white to darker shades of black gave 8% reduced values of drag for higher values of temperature (Hassanalian, Throneberry, et al., 2018b). Wings with black upper and white lower surface (Hassanalian et al., 2018b) or both surfaces in black showed higher values of drag reduction than wings with white upper and black lower surface or both surfaces in white colour. Wing surface with a darker colour like black (Pellerito et al., 2019) can absorb heat up to 50% more than wing surface with a lighter colour like white. High performance is observed for operations at low AoA.

Optimality in aerodynamic and aero-acoustic performance (Brown & Vos, 2018) is exhibited by a blended wing body (BWB). It also exhibits energy efficiency. Airfoil like properties of the fuselage (Lyu & Martins, 2014) aids in wetted area reduction which in turn reduces the drag forces acting on the body. Subsonic efficiency is a characteristic property of this design. Also, not only is the value for skin friction drag decreased but due to smooth intersections between different parts as between the fuselage and the wing, interference drag values also exhibit a trend of decreasing values. Stress reduction (Salazar et al., 2015) is exhibited by a blended wing body. Enhancement in the lift to drag ratio is also observed along with weight efficiency. BWB (Kuntawala, n.d.) is characterized by a streamlined structure. Reduced structural weight and reduction of bending moments in terms of magnitude is also seen. An efficient combination (Yeo & Johnson, 2009) of vertical takeoff and landing with a cruise flight having higher speed values can be achieved using a tilt rotor design. Aerodynamic interference is being used for efficient performance calculations. The interference between the rotor and the wing is of crucial importance in terms of aerodynamic performance as it determines the effect the direction of rotor rotation. An accurate analysis of the interferences between wing-rotor, rotor-rotor and wing-wing is crucial for aerodynamic performance. These aerodynamic interactions would have significant effects on the hover performance. In a conventional tilt rotor, the L/D ratio will be enhanced due to the interferences. Decreased values of induced power and induced velocities are also observable. The L/D ratio is also influenced by the rotor rotational direction. But in a quad tilt rotor, the trend varies. Degradation in the aerodynamic performance is observed due to the interferences and in turn a decrease in the values of L/D ratio is observed. The W/S shows increased values.

Methodology

Demand for unmanned aerial vehicles (UAVs) is increasing as their applications are increasing. The two main applications of drones are in military and civilian sectors. The UAVs have numerous applications. Fascinated by birds, researchers are trying to incorporate their aerodynamic efficiency in UAVs. After studying and analyzing different birds, we concluded that the albatross will be

beneficial for our UAV. Reasons to choose the albatross are – efficiency, color combination, wing profile, and it can soar up to miles without the need to return to land. Wing of our UAV is inspired by the albatross, so we traced the wing profile of albatross as there is less formation of wing tip vortices and we also incorporated the BSLD. As airfoil is a crucial component of wing and the generation of lift is based on the type airfoil we choose, we opted to go with the GOE (173). It is an airfoil inspired by the albatross and the results obtained were good. Aspect Ratio – AR $\propto$ 1/Area, i.e., the larger the aspect ratio smaller is the area of wing surface. The albatross has an aspect ratio of 15.

1. Mechanism Selection- For VTOL transmission we have options- Tilt rotor or tilt wing configuration. Tilt Rotor mechanism is used in the UAV as it consumes very less amount of energy compared to tilt wing. The reason is that tilt rotor produces very less vibrations compared to tilt wing.
2. Design- After concluding every part of UAV we designed the CAD model of UAV in Fusion 360 keeping the dimensions as

Table 1

Dimensions

1]	Span- 2m
2]	Root Chord – 0.3803m
3]	Tip Chord – 0.0255m
4]	Area of the wing – 0.14512*2 m^2
5]	Aspect Ratio – 13.78 Horizontal Stabilizers – a) Root chord – 0.128 m b) Span of H.T. – 0.652m
6]	Vertical Stabilizers – a) Root Chord – 0.15m b) Tip Chord – 0.11m
7]	Taper Ratio –0
8]	Fuselage – 0.9 m
9]	Airfoil – GOE (173)
10]	Propeller Dimensions- 12 inches

XFLR5 software is used to measure the produced lift coefficient (Cl), drag coefficient (Cd), and lift to drag coefficient (Cl/Cd) versus angle of attack (AoA) for similar flight conditions to research the aerodynamic efficiency of the shown

wings. Ring Vortex Lattice Methods (VLM), and 3D-Panel approach are used to conduct aerodynamic studies. These approaches and results between different shapes of wings are compared and presented.

Aerodynamic Analysis

Introduction to Analysis Methodology

Analysis of Albatross aircraft design is completed with the help of two software's, namely Simscale and Xflr5. One is a cloud based CFD solver and other is based on lifting line theory, Vortex lattice method and 3D Panel Method. Aerodynamic analysis here includes particle behavior analysis, surface analysis and the Lift Coefficient, Drag Coefficient, Cl/Cd versus Angle of Attack analysis based on RVLMin respectively.

The vortex lattice method (VLM) is a numerical method used in the analysis of fluid particles around any object. This method considers the wing as extremely thin sheets of surface and computes the lift and induced drag corresponding to it. However, viscosity and thickness of the wing is neglected but it provides fairly considerable lift induced drag and lift coefficient and a comparison can be modeled between different wing bodies.

Analysis in SimScale

For the analysis in SimScale, IGES file of the aircraft model is imported. Since the body is symmetrical about XY plane, it is cut to half for lesser computation time. An enclosure is made around the model representing a virtual wing tunnel and air particles are allowed to travel through the tunnel. The initial conditions were set as: Gauge Pressure = 0, Velocity = 0 (in all three directions), Turb. Kinetic Energy = $3.75e-5$ m^2/s^2, and specific dissipation rate as 3.375 $1/s$. The boundary conditions for the test were set up as an inlet velocity of 15 m/s, pressure outlet with 0 Pascal, one symmetry wall and other as slip walls. Model is considered as a non-slip wall. For precise results, the iteration time is set as 1000 s and maximum runtime is set as $1e+4$ s and a convergence point are printed in graph every sec. Meshing algorithm is set to Hex-Dominant meshing with a predefined automatic meshing of very fine category. Since, mesh quality was fine and better on visualization, no further refinements are given. Then the simulation is started with 0-degree angle of attack.

Results

In solution fields, the model is checked for particle trace and pressure force at different probe points in the model surface.
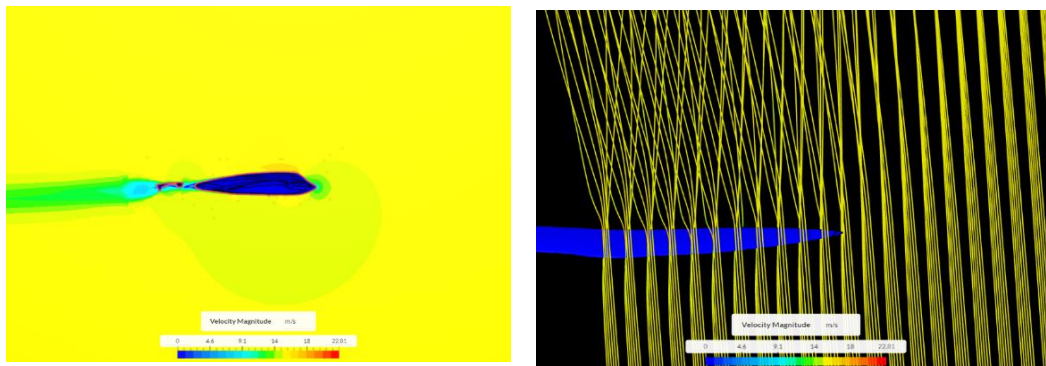
Figure 3

Simscale Analysis
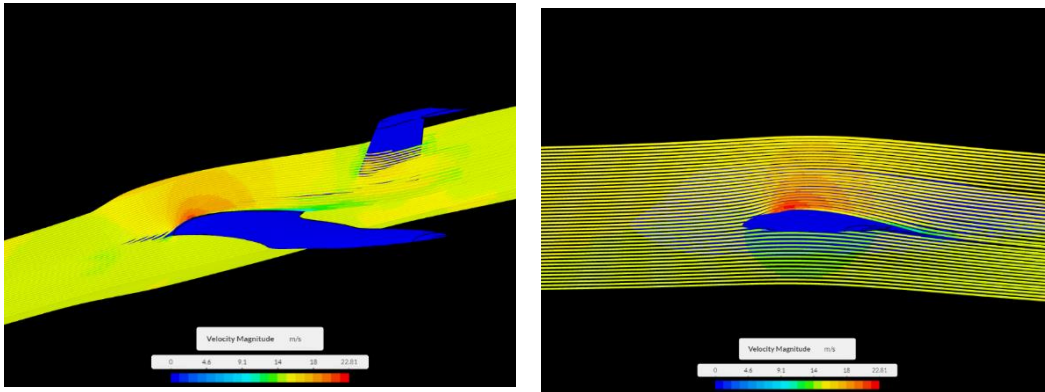
(a) Particle trace analysis of fuselage

(b) Particle trace analysis of aerofoil


(c) Plane velocity contour

(d) Particle trace analysis of wing-tips

The particle trace analysis concluded the flow to be streamlined on 70% of the surface of the model. Due to back thruster, there appears a little turbulent and very high-pressure region in Figure 3 which can be modified. Wingtip vortices generation was negligible at zero AOA. However, after looking at the probe points it is concluded that the design is self-stabilizing in nature, as the stabilizers were producing higher pressures on top surface and lower pressure on bottom surface and vice versa in wing. With a greater pressure difference at the root chord and gradually decreasing towards the wingtip following bell shaped lift distribution presented in upcoming paragraphs. Some pressure probes on the body

of the fuselage resembled the characteristics of a lifting body. Moreover, due to forward sweep given to half of the wing profile there came very less side slip of air particles, creating very high downwash on the rear of the wing and maximum lift. Side slip occurred on the rest of the wings as usual because of the back sweep provided.

Figure 4

*Pressure Probe Points at Different Locations on the Model Surface*
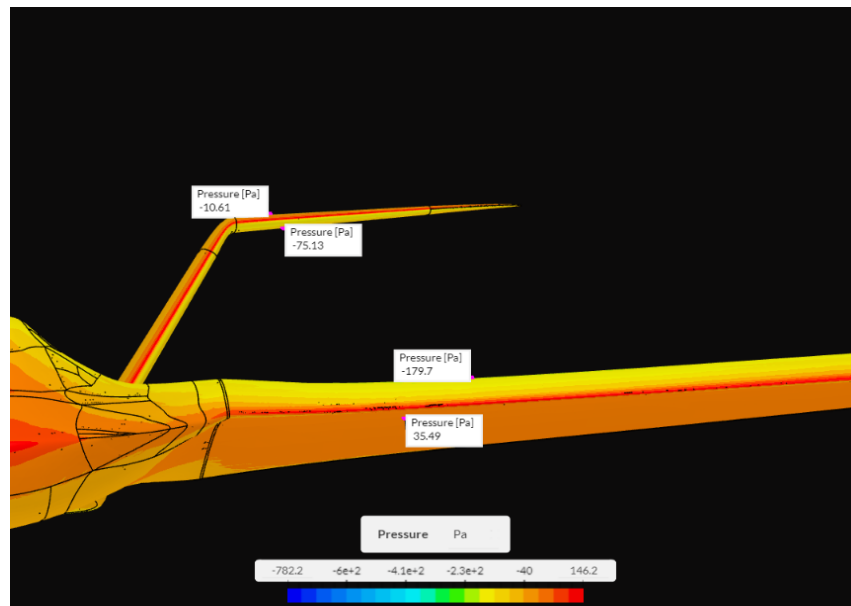
Analysis in XFLR5

Panels and Modeling

In XFLR5, a replica of the design was modeled with same airfoil, twist and span with a wingspan of 2 meters and projected wing area of 0.44 m^2. For proper and precision analysis, the number of mesh elements generated is 4180 also shown in figure. The wing is defined with a mass of 200g assumed (assumption taken as if the model is created with the help of foam). No other masses are assumed to be on the body of the wing. Xflr5 auto-calculates the center of gravity (CoG) and inertia in CoG frame which is used in analysis. The center of gravity comes out to be in right place, nearby one third of the wing. An analysis is created with type 1 category, where a fixed velocity given by user becomes a constraint for other variables. Continuing with Ring Vortex Lattice Method (VLM2) and viscous effect tapped on. Inertia is taken as generated above and analysis is set for sea level conditions with no ground effect and no extra drag.
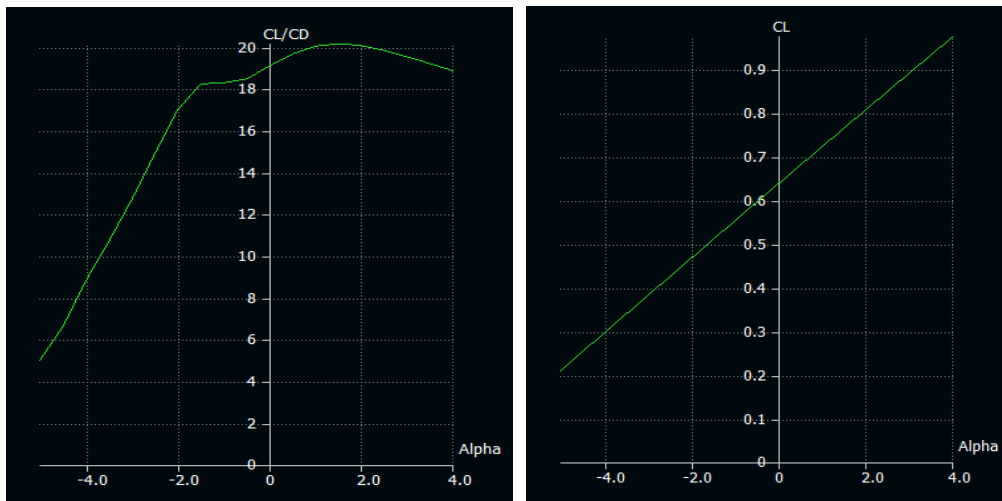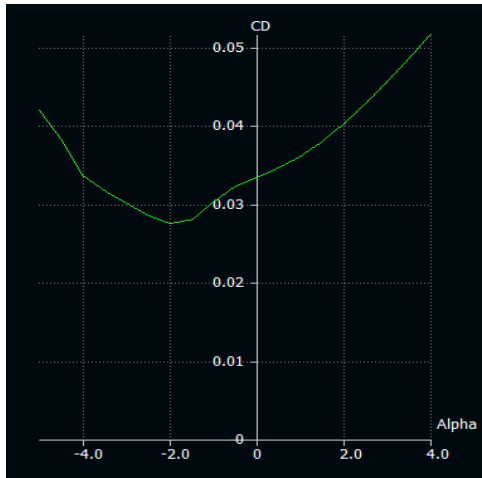
Figure 5

Panel Modeling in XFLR5
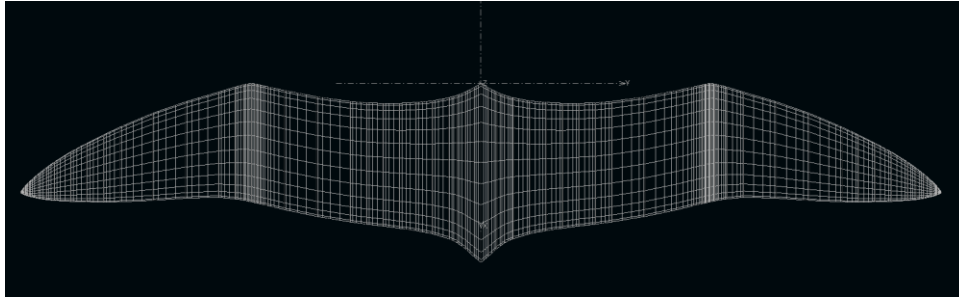
Results

Wing is tested for AOA -5° to 4.5° and the generated data is as expected. At 0° AOA we got a CL of 0.65, A maximum Cl/Cd of about 20 at 1.6°, Minimum Cd of 0.027 at -2°. Concluding with an efficient cruise mode at -2° with a Cl of 0.5 and a minimum Cd of 0.027. The data obtained is understandable when compared to an article given by Stempeck et al. (2018).

Figure 6

Aerodynamic Performance Evaluation of GOE 173Incorporated in the Wing Model
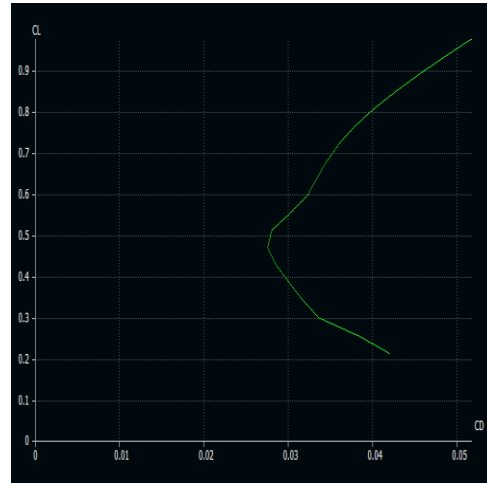

(a) Cl/Cd vs AoA   (b) Cl vs AoA
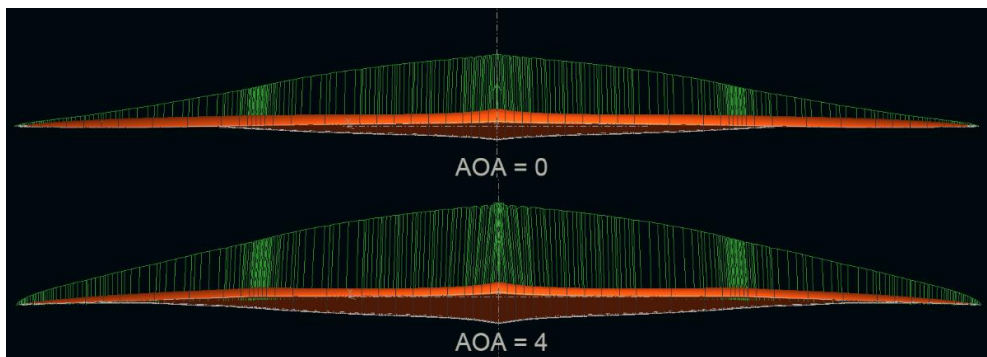
(c) Cd vs AoA   (d) Cl vs Cd

Lift Distribution

When obtaining the lift distribution of the designed wing the outcome is purely Bell-Shaped Lift Distribution. Below is the figure displaying lift distribution at 0° and at 4°AoA. Thus, achieving a milestone to present BSLD with the help of planform and twist across the span. Here wing produces nearly zero lift at the wingtips which is the cause of negative AoA at wingtips and zero taper ratio of wing.

Figure 7

Lift Distribution at AoA=O Degrees and 4 Degrees

Figure 8

Pressure Direction in Vector Form

Pressure Distribution, Streamlines and Up-Down-Washes

The figure displays the pressure distribution in the wing in vector form at different position in the wing. A high low-pressure region is visible at the top root chord following with less value at the tip. One can observe an up-wash production near the wingtip zone as a result of BSLD. Transition from downwash to up wash occurs in the mid of the half span being another reason for low vortex formation. Data is collected at 0° AOA.

Figure 9

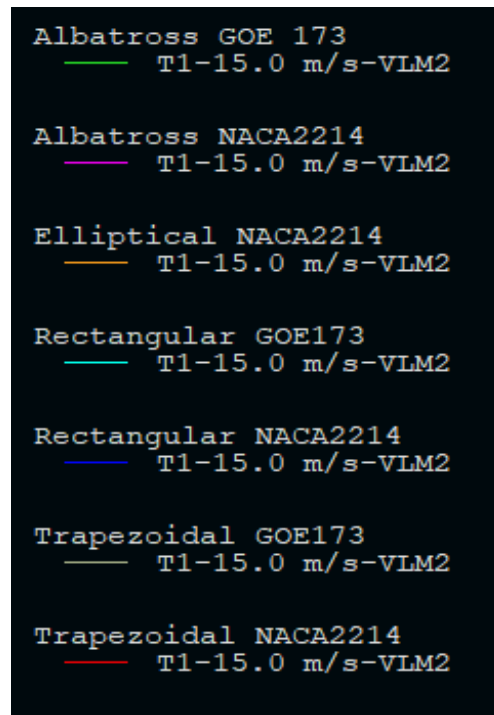*Streamlines and Generation of Up wash and Downwash on the Wing Model*

Comparison With Other Planforms and Airfoil

Approach

In this section the Albatross wing is compared with Rectangular and Trapezoidal planform with GOE 173 airfoil and with Elliptical, Rectangular, Trapezoidal and Albatross wing itself with NACA 2214 airfoil. Analysis for all other planforms are taken with same weight and area configurations and computed for the same prerequisites, Cl, Cd, Cm, and Cl/Cd versus Alpha with same wind speed as 15m/s and are shown in table format for better understanding. Naming for each planform with airfoil is provided in Figure10 Airfoil name for particular planform is depicted after the planform type.

Figure 10

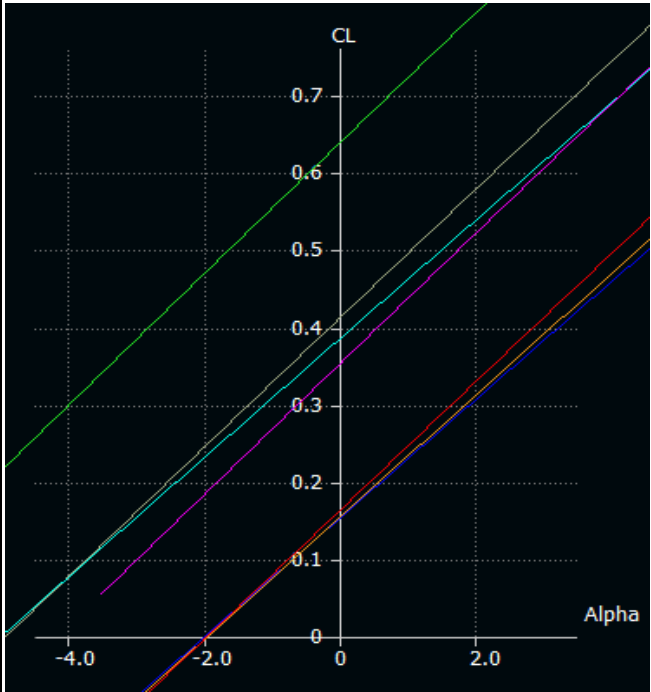*Nomenclature of Different Wing Models for Comparison*

Results and Comparison

| Characteristics	Description
Figure 11 *Cl vs AoA comparison* In comparison the lift follows: Albatross GOE173 > Trapezoidal GOE173 > Rectangular GOE173 > Albatross NACA4412 > Trapezoidal NACA 4412 >Elliptical NACA4412 > Rectangular NACA4412.	Albatross planform with GOE 173 airfoil gives maximum Coefficient of Lift 0.65 at 0° AOA as obvious nature of a high cambered airfoil. But when compared with other plan forms of same area and airfoil. It gives a much better result whereas albatross with NACA 4412 airfoil lies in range of Rectangular and Trapezoidal range with GOE 173 airfoil. Thus, this provides us the capability to carry large payloads.

Figure 12

Cd vs AoA comparison
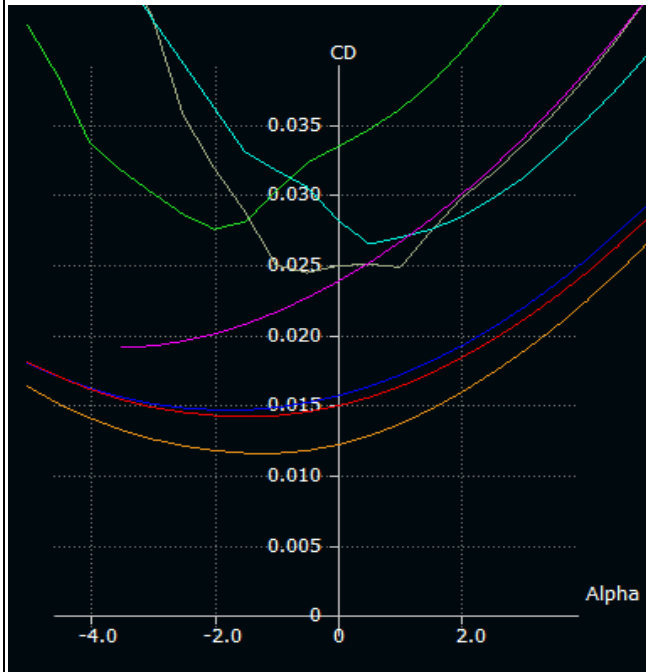
As the airfoil gives much CL at higher AOA. Thus, as usual due to high camber the Albatross GOE173 gives quite higher CD than other GOE 173 planforms. But at negative AOA such as -2º it provides much less drag than others with GOE173 with a positive lift. Thus, -2º can be said as the cruising AOA with a positive CL and much less drag.

However, in drag analysis Elliptical planform with NACA 4412 gives a minimum drag of 0.012 at -1º AOA. But in compensation the least amount of lift also.

Figure 13

Cl/Cd vs AoA
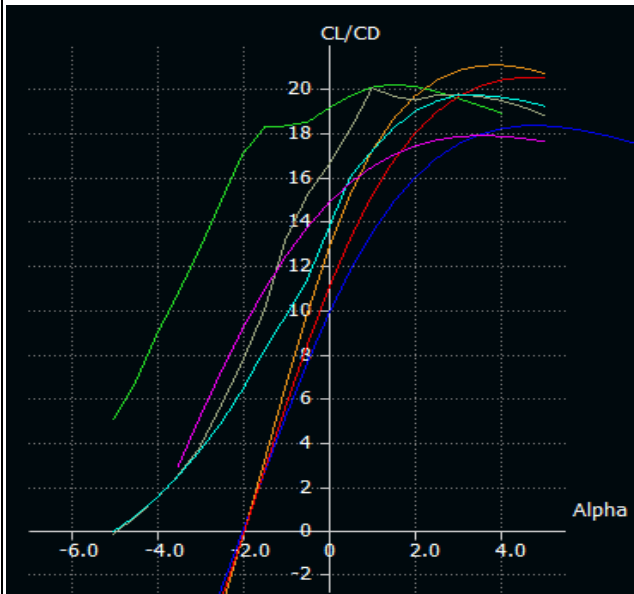
In this context, the highest value is of Elliptical wing of 21 but in negative AOA it collapses rapidly causing quick dive in negative AOA. Then comes the Trapezoidal wing with nearly 20.3 Cl/Cd value, which is also acting same as elliptical. After which Albatross provides a quite uniform flight conditions even in negative AOA and decreasing after -2° with a gradual gradient.
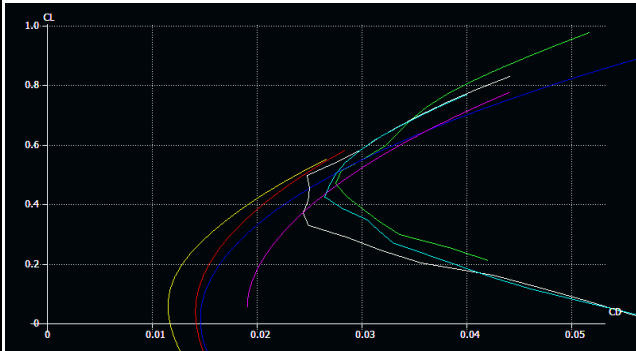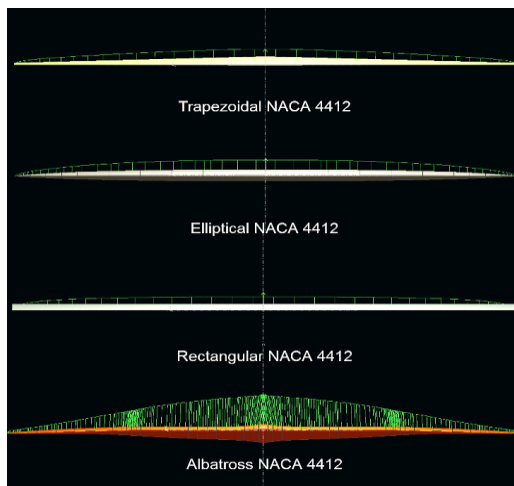
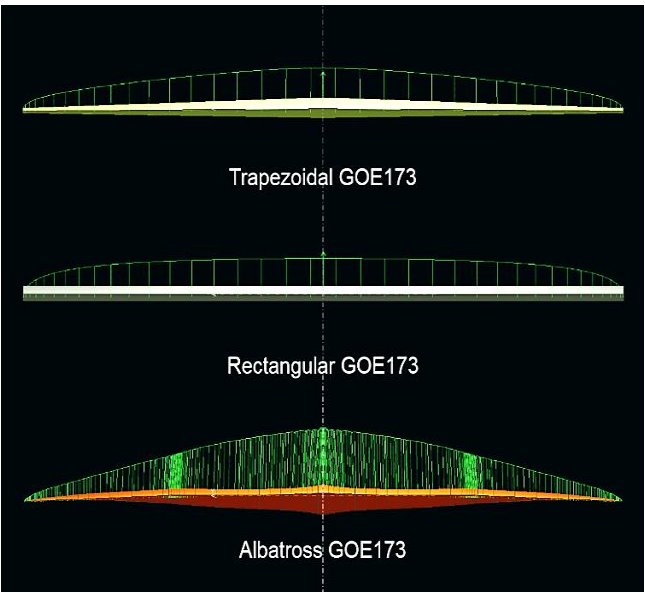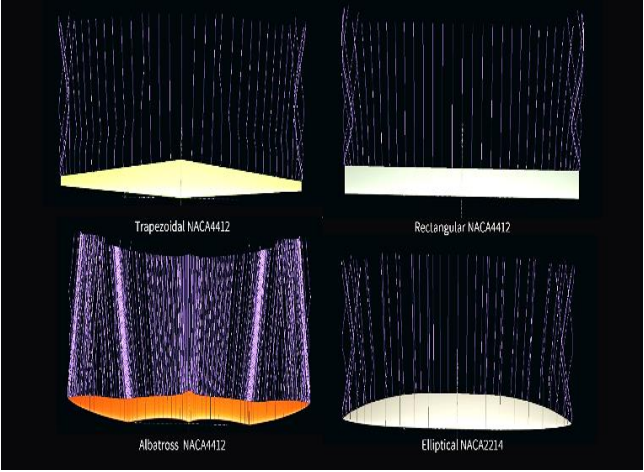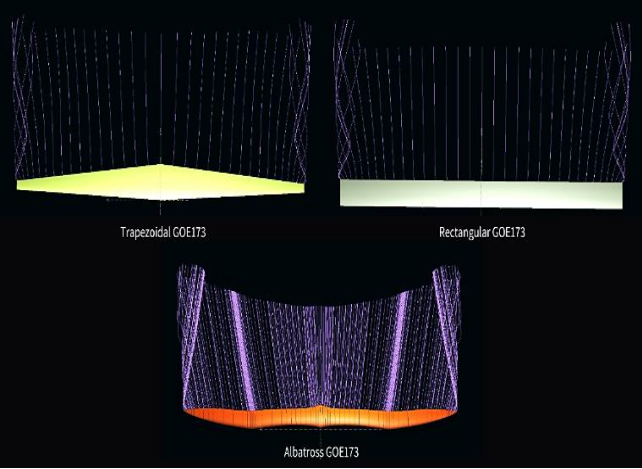|	
Figure 14 *Cl vs Cd* 	The Cl versus Cd graph depicts all the planform with GOE 173 airfoil producing high Cl at with little higher drag in comparison with others. For aircrafts that demands high lift during cruise GOE 173 appears to be a much better airfoil for them.
Figure 15 *Lift distribution – NACA 4412* 	Lift distribution of all NACA 4412 planforms when compared, demonstrated the BSLD effect and Elliptical lift Distribution effect. Image shown in fig.15 lift distributions are shown at 4° AOA. Despite of different planforms, the projected wing area, span and weight

	being same for all. The
The sequence follows: Albatross > Elliptical > Trapezoidal > Rectangular.	Albatross planform outperforms the lift generation following bell shaped lift distribution.
Figure 16 *Lift distribution – NACA GOE 173* 	GOE 173 is high cambered thin airfoil thus a higher lift generation can be observed in this particular combination. And also, the distribution difference between lift of elliptical and BSLD is clearlyvisible. The lift distribution of rectangular wing comes to be a straight line and decreasing near the tips in elliptical manner, causing the production of wingtip vortices. However, in trapezoidal it is kind of

	mixed of bell shaped for 2/3 of the wing and at the end it is elliptical. The opposite happens in Albatross planform. The lift distribution is bell shaped and at/near the tips there is very low lift generation when compared to others. Thus, a cause of less wingtip vortices generation.
Figure 17 *Wingtip vortex formation NACA 4412* 	To reduce wingtip vortices one can put winglets in it. Otherwise can reduce the lift generation at the wingtips. Here, reducing the lift generation by giving zero taper ratio and providing BSLD lift generation we can minimize the wingtip vortex generation to the minimums

The sequence follows: Rectangular > Elliptical > Trapezoidal > Albatross.	can be seen in albatross planform. However, taking into consideration only one would not solve the problem as depicted in elliptical planform (Streamlines are taken at 4° AOA).
Figure 18 *Wingtip vortex formation GOE 173* More the pressure difference, stronger the wingtip vortices.	In GOE 173 airfoil plan forms, we observe the same series as in NACA 4412 plan forms. The highest with Rectangular and Least with Albatross (Streamlines are taken at 4° AOA). But the difference is in the strength of vortices. Since, GOE 173 is a high cambered airfoil thus due to higher pressure difference it creates more strong wingtip vortices.

Conclusions

In biomimicry, Albatross dominates in its endurance and range attracting the focus of researchers to study it. Similarly, to trying to increase the efficiency of current UAV aircraft we designed a design that could serve high lift generation for long range and endurance with optimum efficiency. The wing design resulted in producing minimum wingtip vortices without the use of any winglet/wingtip devices.

The wing when compared to other plan forms with two airfoils NACA 4412 and GOE 173 overcomes other designs in CL/CD, achieving Bell Shaped Lift Distribution, streamlined flow in low Reynolds Number group and wingtip vortices generation. However, as higher lift generation it generated little higher drag when compared to other plan forms which is usual as due to high camber value. This wing configuration fits well in long range and endurance surveying UAV's providing ability to smoothly fly during its mission.

Bio-mimicking is an interesting field where new designs are studied to improve the current technological scenario and has a great future, as bio-species have adapted the environment to take the best out of it. And still we can learn a lot from them.

References

Bowers, A. H., Murillo, O. J., Red, R., Jensen, Eslinger, B., & Gelzer, C. (2016). *On wings of the minimum induced drag: Spanload implications for aircraft and birds*. http://www.sti.nasa.gov

Brown, M., & Vos, R. (2018). Conceptual design and evaluation of blended-wing-body aircraft. *AIAA Aerospace Sciences Meeting, 2018*, *210059*. https://doi.org/10.2514/6.2018-0522

Hassanalian, M., Abdelmoula, H., Ben Ayed, S., & Abdelk, A. (2017a). Effects of birds' wing color on their flight performance for biomimetic purposes. *25th AIAA/AHS Adaptive Structures Conference, 2017*. https://doi.org/10.2514/6.2017-0296

Hassanalian, M., Abdelmoula, H., Ben Ayed, S., & Abdelkefi, A. (2017b). Thermal impact of migrating birds' wing color on their flight performance: Possibility of new generation of biologically inspired drones. *Journal of Thermal Biology*, *66*, 27–32. https://doi.org/10.1016/j.jtherbio.2017.03.013

Hassanalian, M., Ayed, S. B., Ali, M., Houde, P., Hocut, C., & Abdelkefi, A. (2018a). Impact of albatross's wing colors on their skin friction drag: Thermal analysis and blasius boundary layer solution. *2018 Atmospheric Flight Mechanics Conference*. https://doi.org/10.2514/6.2018-2829

Hassanalian, M., Ayed, S. B., Ali, M., Houde, P., Hocut, C., & Abdelkefi, A. (2018b). Insights on the thermal impacts of wing colorization of migrating birds on their skin friction drag and the choice of their flight route. *Journal of Thermal Biology*, *72*, 81–93. https://doi.org/10.1016/j.jtherbio.2018.01.011

Hassanalian, M., Throneberry, G., Ali, M., Ayed, S. B., & Abdelkefi, A. (2018a). Role of wing color and seasonal changes in ambient temperature and solar irradiation on predicted flight efficiency of the Albatross. *Journal of Thermal Biology*, *71*, 112–122. https://doi.org/10.1016/j.jtherbio.2017.11.002

Hassanalian, M., Throneberry, G., Ali, M., Ayed, S. B., & Abdelkefi, A. (2018b). Wing color and drag reduction of albatross-inspired air vehicles. *2018 Aviation Technology, Integration, and Operations Conference*. https://doi.org/10.2514/6.2018-3901

Hospodář, P., & Drábek, A. (n.d.). *Comparison of aerodynamic characteristics provided by wing with bell shaped lift distribution and generalized wings*. https://doi.org/10.1051/matecconf/201930402005

Hunsaker, D. F., & Phillips, W. F. (2020). Ludwig prandtl's 1933 paper concerning wings for minimum induced drag, translation and commentary. *AIAA Scitech 2020 Forum*, *1 PartF*, 1–12. https://doi.org/10.2514/6.2020-0644

Kuntawala, N. B. (n.d.). *Aerodynamic shape optimization of a blended-wing-body aircraft configuration*. ://oddjob.utias.utoronto.ca/dwz/Miscellaneous/

NimeeshaASM2011_FINAL.pdf

Lyu, Z., & Martins, J. R. R. A. (2014). Aerodynamic design optimization studies of a blended-wing-body aircraft. *Journal of Aircraft*, *51*(5), 1604–1617. https://doi.org/10.2514/1.C032491

Newton, L. J. (2019). Stability and control derivative estimation for the bell-shaped lift distribution. *AIAA Scitech 2019 Forum*. https://doi.org/10.2514/6.2019-0157

Nielsen, J. N., & Schwind, R. G. (1971). Decay of a vortex pair behind an aircraft. In *Aircraft Wake Turbulence and Its Detection* (pp. 413–454). Springer. https://doi.org/10.1007/978-1-4684-8346-8_23

Panagiotou, P., Ioannidis, G., Tzivinikos, I., & Yakinthos, K. (2017). Experimental investigation of the wake and the wingtip vortices of a UAV model. *Aerospace*, *4*(4), 53. https://doi.org/10.3390/aerospace4040053

Pellerito, V., Hassanalian, M., Sedaghat, A., Sabri, F., Borvayeh, L., & Sadeghi, S. (2019). Performance analysis of a bioinspired albatross airfoil with heated top wing surface: experimental study. *AIAA Propulsion and Energy Forum and Exposition, 2019*. https://doi.org/10.2514/6.2019-4319

Richter, J., Hainline, K., Louis, S., Agarwal, R. K., Richter, J. , & Hainline, K. ; (n.d.). *Examination of proverse yaw in bell-shaped spanload aircraft*. https://openscholarship.wustl.edu/mems500/91/

Salazar, O. V., Weiss, J., & Morency, F. (2015). *Development of blended wing body aircraft design*. http://aero2015.exordo.com/files/papers/216/final_draft/216_Velazquezsalazar_etal_AERO2015.pdf

Stempeck, A., Hassanalian, M., & Abdelkefi, A. (2018). Aerodynamic performance of albatross-inspired wing shape for marine unmanned air vehicles. *2018 Aviation Technology, Integration, and Operations Conference*. https://doi.org/10.2514/6.2018-3899

Thomas, D.-B., Bachmann, W., Wagner, H., & Baumgartner, W. (2010). *Anatomical, morphometrical and biomechanical studies of barn owls' and pigeons' wings*.https://www.semanticscholar.org/paper/Anatomical%2C-morphometrical-and-biomechanical-of-and-Bachmann-Wagner/ef7c44e1fdf4363fa091f103c3b472f5590ab6e6

Yeo, H., & Johnson, W. (2009). Performance and design investigation of heavy lift tilt-rotor with aerodynamic interference effects. *Journal of Aircraft*, *46*(4), 1231–1239. https://doi.org/10.2514/1.40102